

Shell-Model Calculations for ${}^{16}_{\Lambda}\text{O}$ and ${}^{17}_{\Lambda}\text{O}$ Using Microscopic Effective Interactions with Σ Degrees of Freedom

Shinichiro Fujii*

RI Beam Factory Project Office, RIKEN (The Institute of Physical and Chemical Research), Wako 351-0198, Japan

Ryoji Okamoto and Kenji Suzuki

Department of Physics, Kyushu Institute of Technology, Kitakyushu 804-8550, Japan

(Dated: November 3, 2018)

Shell-model calculations in a large model space are performed for ${}^{16}_{\Lambda}\text{O}$ and ${}^{17}_{\Lambda}\text{O}$. Effective interactions with degrees of freedom of Σ in addition to Λ and nucleons are derived from hyperon-nucleon and nucleon-nucleon interactions within the framework of the unitary-model-operator approach. Effects of the Σ degrees of freedom and the parity-mixing intershell coupling on the Λ hypernuclear structure are investigated, employing the Nijmegen NSC97a-f and NSC89 hyperon-nucleon potentials.

PACS numbers: 21.80.+a, 21.60.Cs, 13.75.Ev, 21.30.Fe

I. INTRODUCTION

One of the challenging problems in theoretical studies of Λ hypernuclei is to describe their properties, starting from hyperon-nucleon (YN) and nucleon-nucleon (NN) interactions given in free space. The nuclear shell-model approach would be one of the promising methods for this problem over a wide range of mass numbers of Λ hypernuclei. In shell-model calculations, however, we need to introduce an effective interaction because of a limited dimension of a shell-model space.

Microscopic derivation of an effective interaction for nuclear shell-model calculations is a fundamental problem for a deeper understanding of nuclei. The G -matrix has often been introduced as an approximate effective interaction, taking into account the state dependence, the medium effect, and the Pauli-blocking effect in a nucleus. Hao *et al.* performed the shell-model calculation for ${}^{16}_{\Lambda}\text{O}$, deriving the ΛN G -matrix for a finite system [1]. Afterward, Tzeng *et al.* have developed their approach to the effective ΛN interaction by calculating core polarization diagrams and folded diagrams [2] in addition to the bare G -matrix [3]. They have also proposed the two-frequency shell model by introducing different frequencies of the harmonic-oscillator (h.o.) wave functions in order to describe different spreads of the wave functions of Λ and nucleons [4].

As for the treatment of the Λ wave function, Motoba has discussed that the mixing of higher nodal h.o. basis functions is needed for the description of the weakly-bound $0p$ states of Λ in the study of ${}^{16}_{\Lambda}\text{O}$ together with ${}^{17}_{\Lambda}\text{O}$ [5, 6], using the YNG interaction proposed by Bandō and Yamamoto [7].

The ${}^{16}_{\Lambda}\text{O}$ is a representative hypernucleus for which experimental data are comparatively accumulated. Fur-

thermore, a high-resolution γ -ray spectroscopy experiment for ${}^{16}_{\Lambda}\text{O}$ has been performed at BNL [8]. Useful information on fine structures reflecting the properties of the underlying YN interactions should be obtained. In such a situation, it is of highly interest to examine to what extent the YN interactions proposed up to now reproduce experimental data on the Λ hypernuclear structure. For this reason, the importance of accurate derivation of the effective interaction for the shell-model calculation has been growing.

In our previous works [9, 10], we have proposed a method for a microscopic description of Λ hypernuclei within the framework of the unitary-model-operator approach (UMOA) [11]. The UMOA is a many-body theory that leads to an energy-independent and Hermitian effective interaction which possesses the decoupling property [12] between two states in a model space and an excluded one. An effective Hamiltonian is given by a unitary transformation of an original Hamiltonian. We here note that this type of effective interaction has been used in recent accurate calculations for light nuclei, for example, the no-core shell model [13] and the method of the effective-interaction hyperspherical harmonics [14].

We applied the UMOA to the calculations of Λ single-particle energies in ${}^{17}_{\Lambda}\text{O}$ and ${}^{41}_{\Lambda}\text{Ca}$ [10], using YN interactions given by the Nijmegen [15, 16] and the Jülich [17] groups. Some reasonable results were obtained, such as the small spin-orbit splitting of Λ [18] compared with those in nuclei though the calculated energies considerably depend on the YN interactions employed. It was also confirmed that the mixing of higher nodal h.o. basis states was important for the description of the Λ wave function.

In this work, we try to perform shell-model calculations for ${}^{16}_{\Lambda}\text{O}$ in addition to ${}^{17}_{\Lambda}\text{O}$. In the shell-model calculations for Λ hypernuclei made so far, the effects of the ΣN channel have been treated as renormalization into a ΛN effective interaction in many cases. The Σ degrees of freedom have not been treated explicitly in the shell-model calculations. Therefore, it is interesting to derive

*Electronic address: sfujii@postman.riken.go.jp

an effective YN interaction which includes not only the ΛN channel but also the ΣN one, and to apply such an effective interaction to shell-model calculations for Λ hypernuclei. Another difference of our approach from the usual shell-model calculations is that we do not employ the experimental single-particle energies of nucleons. Instead, we use the calculated single-particle energies of nucleons which are determined with the effective NN interactions. We also use the single-particle energies of Λ and Σ determined in a similar way.

This paper is organized as follows. In Sec. II, the procedure for the shell-model calculation is given. The calculated results for ${}^{\Lambda}_{\Lambda}{}^{17}\text{O}$ and ${}^{\Lambda}_{\Lambda}{}^{16}\text{O}$ using the Nijmegen soft-core 97 (NSC97) [16] and NSC89 [15] potentials are shown in Sec. III. Finally, concluding remarks are made in Sec. IV.

II. CALCULATION METHOD

A. Effective Hamiltonian

We first consider a Hamiltonian of a hypernuclear system consisting of nucleons and one Λ (or Σ). It may be written in the second-quantization form as

$$\begin{aligned} H = & \sum_{\alpha\beta} \langle \alpha | t_N | \beta \rangle c_{\alpha}^{\dagger} c_{\beta} + \frac{1}{4} \sum_{\alpha\beta\gamma\delta} \langle \alpha\beta | v_{N_1 N_2} | \gamma\delta \rangle c_{\alpha}^{\dagger} c_{\beta}^{\dagger} c_{\delta} c_{\gamma} \\ & + \sum_{\mu\nu} \langle \mu | t_Y + \Delta m | \nu \rangle d_{\mu}^{\dagger} d_{\nu} \\ & + \sum_{\mu\alpha\nu\beta} \langle \mu\alpha | v_{YN} | \nu\beta \rangle d_{\mu}^{\dagger} c_{\alpha}^{\dagger} c_{\beta} d_{\nu}, \end{aligned} \quad (1)$$

where c^{\dagger} (c) is the creation (annihilation) operator for a nucleon in the usual notation, and d^{\dagger} (d) is the creation (annihilation) operator for a hyperon, Λ or Σ . The kinetic energies of a nucleon and a hyperon are denoted by t_N and t_Y , respectively. The quantities $v_{N_1 N_2}$ and v_{YN} represent the NN and YN interactions, respectively. The symbols α, β, γ , and δ are used for the sets of quantum numbers of nucleon states, and μ and ν for those of hyperon states. The $|\alpha\beta\rangle$ is the anti-symmetrized and normalized two-body NN state. The term Δm denotes the difference between the rest masses of Λ and Σ .

In order to properly treat the short-range two-body correlation, we introduce a unitary transformation of the Hamiltonian as

$$\tilde{H} = e^{-S} H e^S, \quad (2)$$

where S is the sum of anti-Hermitian two-body operators for the NN and YN systems defined as

$$S = S^{(NN)} + S^{(YN)}, \quad (3)$$

with

$$S^{(NN)} = \frac{1}{4} \sum_{\alpha\beta\gamma\delta} \langle \alpha\beta | S_{N_1 N_2} | \gamma\delta \rangle c_{\alpha}^{\dagger} c_{\beta}^{\dagger} c_{\delta} c_{\gamma}, \quad (4)$$

$$S^{(YN)} = \sum_{\mu\alpha\nu\beta} \langle \mu\alpha | S_{YN} | \nu\beta \rangle d_{\mu}^{\dagger} c_{\alpha}^{\dagger} c_{\beta} d_{\nu}. \quad (5)$$

We adopt a cluster expansion of the unitarily transformed Hamiltonian as

$$\tilde{H} = \tilde{H}^{(1)} + \tilde{H}^{(2)} + \dots, \quad (6)$$

where the first two terms are written explicitly as

$$\tilde{H}^{(1)} = \sum_{\alpha\beta} \langle \alpha | h_N | \beta \rangle c_{\alpha}^{\dagger} c_{\beta} + \sum_{\mu\nu} \langle \mu | h_Y | \nu \rangle d_{\mu}^{\dagger} d_{\nu}, \quad (7)$$

$$\begin{aligned} \tilde{H}^{(2)} = & \frac{1}{4} \sum_{\alpha\beta\gamma\delta} \langle \alpha\beta | \tilde{v}_{N_1 N_2} | \gamma\delta \rangle c_{\alpha}^{\dagger} c_{\beta}^{\dagger} c_{\delta} c_{\gamma} \\ & - \sum_{\alpha\beta} \langle \alpha | u_N | \beta \rangle c_{\alpha}^{\dagger} c_{\beta} \\ & + \sum_{\mu\alpha\nu\beta} \langle \mu\alpha | \tilde{v}_{YN} | \nu\beta \rangle d_{\mu}^{\dagger} c_{\alpha}^{\dagger} c_{\beta} d_{\nu} \\ & - \sum_{\mu\nu} \langle \mu | u_Y | \nu \rangle d_{\mu}^{\dagger} d_{\nu}. \end{aligned} \quad (8)$$

Since the exponent S in Eq. (2) is a two-body operator, the one-body parts in \tilde{H} are unchanged and given by

$$h_N = t_N + u_N, \quad (9)$$

$$h_Y = t_Y + u_Y + \Delta m_Y. \quad (10)$$

The terms u_k for $k = N$ and Y are the auxiliary single-particle potentials of a nucleon and a hyperon, respectively, and at this stage they are arbitrary. The quantities \tilde{v}_{kl} for $\{kl\} = \{N_1 N_2\}$ and $\{YN\}$ are the transformed two-body interactions for the NN and YN systems, and they are given by

$$\begin{aligned} \tilde{v}_{N_1 N_2} = & e^{-S_{N_1 N_2}} (h_{N_1} + h_{N_2} + v_{N_1 N_2}) e^{S_{N_1 N_2}} \\ & - (h_{N_1} + h_{N_2}), \end{aligned} \quad (11)$$

$$\begin{aligned} \tilde{v}_{YN} = & e^{-S_{YN}} (h_Y + h_N + v_{YN}) e^{S_{YN}} \\ & - (h_Y + h_N). \end{aligned} \quad (12)$$

In nuclear many-body problems, it is important how to choose the auxiliary potential u_k . We introduce u_N and u_Y as self-consistent potentials defined with the transformed two-body interactions $\tilde{v}_{N_1 N_2}$ and \tilde{v}_{YN} as

$$\langle \alpha | u_N | \beta \rangle = \sum_{\xi \leq \rho_F} \langle \alpha \xi | \tilde{v}_{N_1 N_2} | \beta \xi \rangle, \quad (13)$$

$$\langle \mu | u_Y | \nu \rangle = \sum_{\xi \leq \rho_F} \langle \mu \xi | \tilde{v}_{YN} | \nu \xi \rangle, \quad (14)$$

where ρ_F is the uppermost occupied level, and the symbol ξ indicates an occupied state for nucleons. If u_N and

u_Y are defined as given in Eqs. (13) and (14), it can be proved that the second and fourth terms on the right-hand side of Eq. (8) are canceled by the contributions of the bubble diagrams of the first and third terms, respectively. Therefore, the cluster terms $\tilde{H}^{(1)}$ and $\tilde{H}^{(2)}$ include only the one- and two-body operators, respectively, if we write them in the normal-product form with respect to particles and holes [11].

The transformed Hamiltonian \tilde{H} contains, in general, three-or-more-body transformed interactions, even if the starting Hamiltonian H in Eq. (1) does not include three-or-more-body interactions. In the previous paper [10], a method of evaluating the three-body cluster (TBC) effect has been presented for the calculation of Λ single-particle energies. The TBC terms are generated as the transformed three-body interactions among the YNN and NNN systems, and they contain generally two factors of the correlation operator S_{kl} for $\{kl\} = \{N_1 N_2\}$ and $\{YN\}$. It has been verified that the matrix elements of the correlation operator are quite small, and thus the TBC contributions to the Λ single-particle energies are considerably smaller than the contributions from the one- and two-body cluster terms. The TBC contributions to the Λ single-particle energies in $^{17}_\Lambda\text{O}$ were found to be at most 4% of the Λ potential energy. Therefore, we assume that the TBC terms do not have significant effects on the energy levels in $^{16}_\Lambda\text{O}$, and the three-or-more-body effective interactions are not included in the present calculation.

B. Model space of two-body NN and YN states

An important problem in the present approach is how to determine the two-body correlation operators S_{kl} for $\{kl\} = \{N_1 N_2\}$ and $\{YN\}$ in Eqs. (4) and (5), respectively. These operators are given as solutions to the equation of decoupling as

$$Q_{kl} e^{-S_{kl}} (h_k + h_l + v_{kl}) e^{S_{kl}} P_{kl} = 0, \quad (15)$$

where P_{kl} and Q_{kl} are projection operators which act in the space of two-body states and project a two-body state onto the low-momentum model space and the high-momentum space, respectively. It has been proved that Eq. (15) for S_{kl} can be solved in a nonperturbative way [9, 11] under the conditions

$$P_{kl} S_{kl} P_{kl} = Q_{kl} S_{kl} Q_{kl} = 0. \quad (16)$$

In order to actually calculate the effective interaction, we need two-body model spaces for the NN and YN channels. We choose the same model space for the NN channel as in Ref. [11]. We here define the model space of the YN channel as follows: Two-body YN states for $Y = \Lambda$ and Σ are given by the product of the h.o. wave functions as

$$|\mu_Y \alpha_N\rangle = |n_Y l_Y j_Y m_Y, n_N l_N j_N m_N\rangle \quad (17)$$

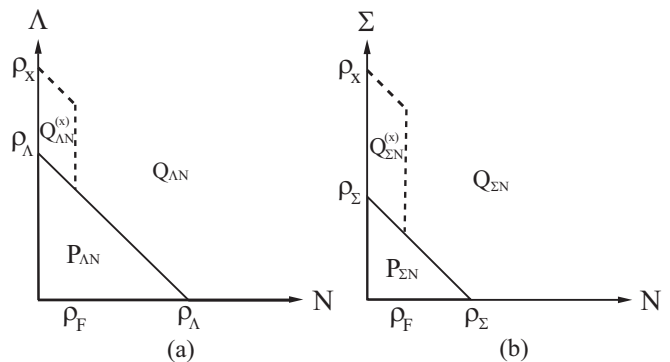


FIG. 1: The model space of the ΛN (a) and ΣN (b) channels and its complement.

with the h.o. quantum numbers, $\{n_Y, l_Y, j_Y, m_Y\}$ and $\{n_N, l_N, j_N, m_N\}$, of a hyperon and a nucleon, respectively. The model space of the YN channel $P_{\Lambda N} + P_{\Sigma N}$ and its complement $Q_{\Lambda N} + Q_{\Sigma N}$ are defined with boundary numbers ρ_Λ and ρ_Σ as

$$|\mu_\Lambda \alpha_N\rangle \in \begin{cases} P_{\Lambda N} & \text{if } 2n_\Lambda + l_\Lambda + 2n_N + l_N \leq \rho_\Lambda, \\ Q_{\Lambda N} & \text{otherwise} \end{cases} \quad (18)$$

and

$$|\mu_\Sigma \alpha_N\rangle \in \begin{cases} P_{\Sigma N} & \text{if } 2n_\Sigma + l_\Sigma + 2n_N + l_N \leq \rho_\Sigma, \\ Q_{\Sigma N} & \text{otherwise.} \end{cases} \quad (19)$$

Note that the numbers ρ_Λ and ρ_Σ are zero or positive integers. In Fig. 1, the model space and its complement are shown. The YN states in the space $Q_{\Lambda N}^{(X)} + Q_{\Sigma N}^{(X)}$ specified by the numbers $\rho_\Lambda, \rho_\Sigma, \rho_F$, and ρ_X in Fig. 1 should be excluded due to the Pauli principle for nucleons, and defined as

$$|\mu_\Lambda \alpha_N\rangle \in Q_{\Lambda N}^{(X)} \quad \text{if } \rho_\Lambda < 2n_\Lambda + l_\Lambda + 2n_N + l_N \leq \rho_X \\ \text{and } 0 \leq 2n_N + l_N \leq \rho_F \quad (20)$$

and

$$|\mu_\Sigma \alpha_N\rangle \in Q_{\Sigma N}^{(X)} \quad \text{if } \rho_\Sigma < 2n_\Sigma + l_\Sigma + 2n_N + l_N \leq \rho_X \\ \text{and } 0 \leq 2n_N + l_N \leq \rho_F. \quad (21)$$

The number ρ_F denotes the highest occupied orbit in the core nucleus and is taken as $\rho_F = 1$ in the present case of ^{16}O . The value of ρ_X should be chosen as large as possible so as to exclude the YN states in the Pauli-blocked $Q_{YN}^{(X)}$ space. In the present calculation, we take as $\rho_X = 12$. The values of ρ_Λ and ρ_Σ , in principle, should be taken as a large value so that the results become independent of ρ_Λ and ρ_Σ . As for ρ_Λ , we take as $\rho_\Lambda = 8$ which has been shown to be sufficiently large in the previous work [9]. The ρ_Σ -dependence of calculated energy levels in $^{17}_\Lambda\text{O}$ and $^{16}_\Lambda\text{O}$ will be discussed in detail in Sec. III.

The effective interaction \tilde{v}_{YN} in Eq. (12) is determined by solving the decoupling equation in Eq. (15) between

the model space $P_{YN} = P_{\Lambda N} + P_{\Sigma N}$ and the space $Q_{YN} = (Q_{\Lambda N} - Q_{\Lambda N}^{(X)}) + (Q_{\Sigma N} - Q_{\Sigma N}^{(X)})$. The detailed procedure for solving the decoupling equation has been given in Ref. [9].

C. Shell-model diagonalization

We proceed to discuss the calculation procedure for the shell-model diagonalization. The shell-model spaces we adopt are given by

$$d_{\Lambda}^{\dagger}|\phi_0\rangle \oplus d_{\Lambda}^{\dagger}a^{\dagger}b^{\dagger}|\phi_0\rangle \oplus d_{\Sigma}^{\dagger}a^{\dagger}b^{\dagger}|\phi_0\rangle \quad (22)$$

for ${}_{\Lambda}^{17}\text{O}$ and

$$d_{\Lambda}^{\dagger}b^{\dagger}|\phi_0\rangle \oplus d_{\Sigma}^{\dagger}b^{\dagger}|\phi_0\rangle \oplus d_{\Lambda}^{\dagger}a^{\dagger}b^{\dagger}b^{\dagger}|\phi_0\rangle \oplus d_{\Sigma}^{\dagger}a^{\dagger}b^{\dagger}b^{\dagger}|\phi_0\rangle \quad (23)$$

for ${}_{\Lambda}^{16}\text{O}$, where d_{Λ}^{\dagger} (d_{Σ}^{\dagger}) is the creation operator of a Λ (Σ), and a^{\dagger} and b^{\dagger} are the creation operators of a particle and a hole, respectively, for nucleons. The state $|\phi_0\rangle$ is the unperturbed ground state of the core nucleus which is the particle-hole vacuum satisfying $a|\phi_0\rangle = b|\phi_0\rangle = 0$.

In general, the transformed Hamiltonian \tilde{H} in Eq. (2) includes three-or-more-body effective interactions. In the present calculation, as mentioned before, we neglect the many-body effective interactions, and take the one- and two-body parts in \tilde{H} . In this approximation, the direct coupling of $d_{\Lambda}^{\dagger}|\phi_0\rangle$ and $d_{\Lambda}^{\dagger}a^{\dagger}b^{\dagger}|\phi_0\rangle$ in ${}_{\Lambda}^{17}\text{O}$ does not occur anymore. This is because the operator $S_{N_1 N_2}$ in Eq. (4) is determined so that the transformed Hamiltonian does not contain interactions inducing two-particle-two-hole ($2p$ - $2h$) excitations in the ground state of the core nucleus [11]. The same discussion applies to the direct coupling of $d_{\Lambda}^{\dagger}b^{\dagger}|\phi_0\rangle$ and $d_{\Lambda}^{\dagger}a^{\dagger}b^{\dagger}b^{\dagger}|\phi_0\rangle$ in ${}_{\Lambda}^{16}\text{O}$. On these considerations, we take only the shell-model spaces as in Eqs. (22) and (23) in which the effective Hamiltonian is diagonalized.

It should be noted that since we diagonalize the unitarily transformed Hamiltonian \tilde{H} in Eq. (2), a true eigenstate of the original Hamiltonian H can be given by a transformed state. That is to say, an eigenstate of H denoted by $|\Psi_k\rangle$ is given by $e^S|\psi_k\rangle$, where $|\psi_k\rangle$ is an eigenstate of the transformed Hamiltonian \tilde{H} . The correlated ground state of the core nucleus $|\Phi_0\rangle$ is related to the unperturbed shell-model ground state $|\phi_0\rangle$ as $|\Phi_0\rangle = e^S|\phi_0\rangle$. In general, $|\Phi_0\rangle$ contains $2p$ - $2h$, $4p$ - $4h$, and higher-order particle-hole components through the unitary transformation e^S with the two-body correlation operator S . In a similar way, the transformed state $|\Psi_k\rangle$ contains many-particle-many-hole components consistently with the correlations in the ground state of the core nucleus.

We here want to discuss the Λ - Σ coupling three-body force of which effect has been pointed out by Tzeng *et al.* [3, 4]. In the present shell-model calculation we neglect the transformed three-or-more-body interactions, but this does not mean to neglect the Λ - Σ three-body

force. In our approach the ΣN - ΛN coupling terms remain in the transformed Hamiltonian, if we include the ΣN states in the YN model space. Therefore, the ΣN - ΛN coupling is evaluated as configuration mixing of Σ -nucleons states into Λ -nucleons ones.

In shell-model calculations, spurious states caused by the center-of-mass (c.m.) motion often mix with physical states. In the present case, the $1p$ - $1h$ spurious $1^-(T=0)$ state in ${}^{16}\text{O}$ affects low-lying physical states, especially, the $3/2^-(T=0)$ and $1/2^-(T=0)$ states in ${}_{\Lambda}^{17}\text{O}$ [19]. In order to remove the spurious c.m. state, we add the following term

$$H_{\beta} = \beta|1^-_{\text{c.m.}}\rangle\langle 1^-_{\text{c.m.}}| \quad (24)$$

to the effective Hamiltonian, and then the Hamiltonian is diagonalized. We take as $\beta = 3\hbar\omega$ in Eq. (24) with the h.o. frequency $\hbar\omega$, and we eliminate the spurious 1^- state from the low-lying states under consideration.

As for the value of $\hbar\omega$, we take as $\hbar\omega = 14\text{MeV}$ because the result tends to the saturation minimum of the binding energy in ${}^{16}\text{O}$ at close this value [20]. We employ the same value 14MeV for $\hbar\omega$ of the hyperons Λ and Σ . In general, the spreads of the wave functions of the hyperons and nucleons are different from each other. If one tries to describe the states of the hyperons and nucleons using the h.o. wave functions, one may choose the different frequencies as done in the two-frequency shell model [4]. In the present work, however, we take the values of $\hbar\omega$ commonly for the hyperons and nucleons, because the final result in the shell-model calculation should be, in principle, independent of $\hbar\omega$ if we take a sufficiently large model space in the calculation.

Since we diagonalize the effective Hamiltonian in the space of the particle-hole states, we should remove unlinked-diagram contributions in a suitable way. In our approach, non-diagonal matrix elements of the one-body part of the nucleon remain in the effective Hamiltonian, which induces the $1p$ - $1h$ excitation and causes the unlinked-diagram effect. In order to remove the unlinked terms, we calculate separately the correlation energy E_c of the core nucleus in the space of $|\phi_0\rangle \oplus a^{\dagger}b^{\dagger}|\phi_0\rangle$. We then subtract E_c from the eigenvalue E_{SM} of the shell-model effective Hamiltonian. In the case of ${}_{\Lambda}^{17}\text{O}$, the value of $E_{\text{SM}} - E_c$ corresponds to the binding energy of Λ measured from the ${}^{16}\text{O} + \Lambda$ threshold.

III. RESULTS AND DISCUSSION

We performed calculations employing the Nijmegen soft-core 97 (NSC97) [16] and NSC89 [15] potentials for the YN interaction. As for the NN interaction, we choose the Paris [21] potential. All the interaction matrix elements of the Hamiltonian in Eq. (2) are derived from these bare interactions within the framework of the UMOA. In these calculations we do not introduce any adjustable parameters and experimental values such as single-particle energies of Λ , Σ , and nucleons. This sort

of microscopic calculation would be worthy of revealing the states of the present YN interactions.

A. Structure of ${}_{\Lambda}^{17}\text{O}$

In Fig. 2, we first show the calculated energy levels in ${}_{\Lambda}^{17}\text{O}$ for the NSC97d and NSC97f potentials as a function of ρ_{Σ} . The results correspond to the Λ single-particle energies including the effect of core polarization. One can see that the results for both potentials are stable for the change of the values of ρ_{Σ} , and almost the same as the results for “ ΛN ”. The “ ΛN ” means that the ΣN channel is not included in the model space. This suggests that the effects of the ΣN channel into the ΛN effective interaction can be well renormalized. It has been confirmed that this tendency of the convergence is also observed for the other NSC97 models.

In Table I, we tabulate the calculated energy levels in ${}_{\Lambda}^{17}\text{O}$ with the values of the Λ spin-orbit splitting for the NSC97a-f potentials. In this table the values for $\rho_{\Sigma} = 5$ are presented as the sets of convergent results in this study, and we also list the values in parentheses which are the results for “ ΛN ” for reference. The results show that the energies for the NSC97c are the most attractive in the NSC97 models, on the other hand, those for the NSC97f are the least attractive. This trend is also seen in the calculation for nuclear matter as in Ref. [16]. We also see that the Λ spin-orbit splittings become larger from the NSC97a to NSC97f. Recently, the magnitude of the Λ spin-orbit splitting in ${}_{\Lambda}^{13}\text{C}$ has been established experimentally as $\Delta E_{ls}({}_{\Lambda}^{13}\text{C}) = E(1/2^-) - E(3/2^-) = 152 \pm 54(\text{stat}) \pm 36(\text{syst})$ keV [18]. Our results of the Λ spin-orbit splitting in ${}_{\Lambda}^{17}\text{O}$ for the NSC97 models may considerably larger than the value suggested from the experimental result of ${}_{\Lambda}^{13}\text{C}$.

We note here that the present results in Table I agree

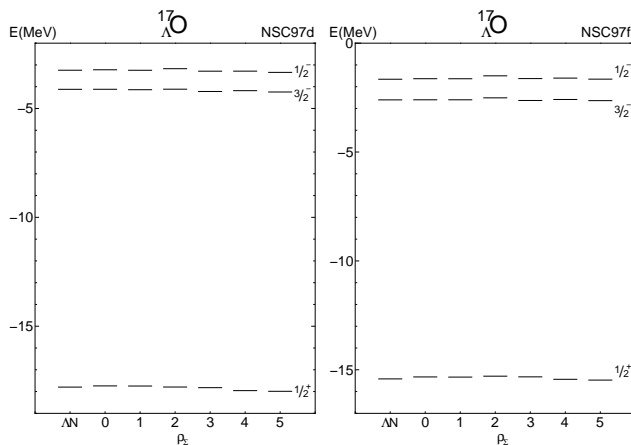


FIG. 2: The calculated energy levels in ${}_{\Lambda}^{17}\text{O}$ for the NSC97d and NSC97f potentials as a function of ρ_{Σ} . The energy levels for “ ΛN ” are the results for the case without the ΣN channel in the model space.

well with those obtained in the previous work [10] in which the calculation was made perturbatively. We may say that both methods, the shell-model diagonalization and the perturbative method, are workable in the calculation of the Λ single-particle energies in Λ hypernuclei which have the simple structure. In the following subsection, we shall proceed to study a more complex system, namely, ${}_{\Lambda}^{16}\text{O}$ by the shell-model diagonalization.

B. Structure of ${}_{\Lambda}^{16}\text{O}$

Experimental energy levels in ${}_{\Lambda}^{16}\text{O}$ are usually relative to the ground state of ${}^{15}\text{O}$. Since we employ the particle-hole formalism, the results of the shell-model diagonalization are relative to the ground state of ${}^{16}\text{O}$. Therefore, we subtract the mass difference between ${}^{15}\text{O}$ and ${}^{16}\text{O}$ from the calculated results in order to compare our results with the experimental spectrum. The mass difference is computed by the shell-model diagonalization in the space of the $1h+(1p-2h)$ configuration, using the nucleon parts of the effective Hamiltonian in Eq. (2).

In Fig. 3, we show the ρ_{Σ} -dependence of the calculated energies for low-lying states in ${}_{\Lambda}^{16}\text{O}$ for the NSC97d and NSC97f. One can see that the energy levels of the negative parity states become slightly more attractive as the value of ρ_{Σ} becomes larger. We may say, however, that the splittings of the ground-stated doublet ($0_1^-, 1_1^-$) hardly change, and thus almost convergent results are obtained. On the other hand, in the first-excited doublet ($1_2^-, 2_1^-$), the splittings become slightly smaller as ρ_{Σ} increases. These trends have also been observed in the results for the other NSC97 models.

There are some arguments that splittings of the spin doublets ($J_{>,<} = J_{\text{core}} \pm s_{1/2}^{\Lambda}$) in Λ hypernuclei depend on the spin-dependent ΛN interactions, such as the spin-spin and tensor interactions [16, 22]. In addition, the ΣN - ΛN coupling may affect not only the magnitude of

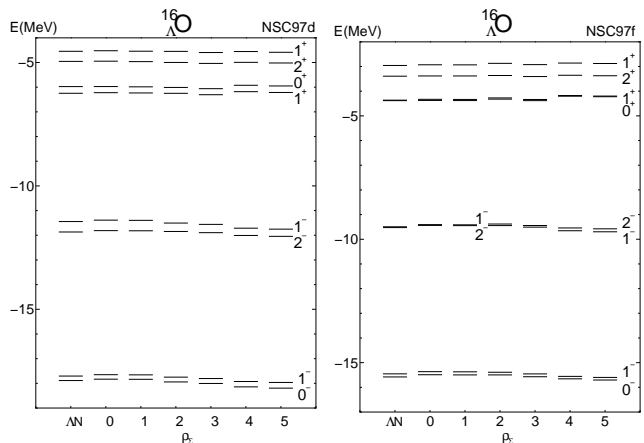


FIG. 3: The ρ_{Σ} -dependence of the calculated results of low-lying states in ${}_{\Lambda}^{16}\text{O}$.

TABLE I: The values of the calculated energy levels in $^{17}\Lambda\text{O}$ for the NSC97a-f potentials for $\rho_\Sigma = 5$. The quantity ΔE_{ls} stands for the magnitude of the Λ spin-orbit splitting defined as $\Delta E_{ls} = E(1/2^-) - E(3/2^-)$. The values in parentheses denote the results using the renormalized “ ΛN ” effective interaction. All energies are in MeV.

	NSC97a	NSC97b	NSC97c	NSC97d	NSC97e	NSC97f
$1/2^-$	-3.29 (-3.44)	-3.19 (-3.37)	-3.51 (-3.67)	-3.24 (-3.34)	-2.82 (-2.87)	-1.65 (-1.65)
$3/2^-$	-3.72 (-3.91)	-3.75 (-3.95)	-4.23 (-4.42)	-4.12 (-4.24)	-3.77 (-3.84)	-2.60 (-2.64)
$1/2^+$	-17.04 (-17.39)	-17.14 (-17.46)	-17.91 (-18.23)	-17.79 (-17.99)	-17.26 (-17.40)	-15.42 (-15.47)
ΔE_{ls}	0.44 (0.47)	0.56 (0.58)	0.72 (0.74)	0.88 (0.90)	0.94 (0.97)	0.95 (0.99)

TABLE II: The calculated energy values of the low-lying states in $^{16}\Lambda\text{O}$ for the NSC97a-f potentials for $\rho_\Sigma = 5$. The quantity $\Delta E_{1,2}$ stands for the magnitude of the splitting between the 1_2^- and 2_1^- states defined as $\Delta E_{1,2} = E(1_2^-) - E(2_1^-)$, and $\Delta E_{1,0}$ is defined as $\Delta E_{1,0} = E(1_1^-) - E(0_1^-)$. The values in parentheses denote the results using the renormalized “ ΛN ” effective interaction. All energies are in MeV.

	NSC97a	NSC97b	NSC97c	NSC97d	NSC97e	NSC97f
1_2^+	-4.38 (-4.26)	-4.38 (-4.25)	-4.80 (-4.69)	-4.59 (-4.55)	-4.15 (-4.17)	-2.88 (-2.96)
2_1^+	-4.50 (-4.36)	-4.58 (-4.43)	-5.13 (-4.99)	-5.02 (-4.95)	-4.63 (-4.61)	-3.37 (-3.39)
0_1^+	-4.98 (-4.86)	-5.16 (-5.04)	-5.90 (-5.80)	-5.95 (-5.98)	-5.63 (-5.72)	-4.22 (-4.38)
1_1^+	-5.67 (-5.60)	-5.76 (-5.70)	-6.38 (-6.32)	-6.21 (-6.25)	-5.74 (-5.83)	-4.20 (-4.36)
1_2^-	-10.74 (-10.25)	-10.93 (-10.45)	-11.77 (-11.32)	-11.75 (-11.44)	-11.33 (-11.08)	-9.70 (-9.50)
2_1^-	-11.69 (-11.39)	-11.71 (-11.43)	-12.36 (-12.08)	-12.04 (-11.87)	-11.43 (-11.31)	-9.58 (-9.53)
1_1^-	-17.24 (-16.85)	-17.34 (-16.96)	-18.14 (-17.76)	-17.96 (-17.71)	-17.43 (-17.23)	-15.60 (-15.45)
0_1^-	-17.93 (-17.48)	-17.93 (-17.51)	-18.57 (-18.12)	-18.20 (-17.89)	-17.57 (-17.32)	-15.70 (-15.58)
$\Delta E_{1,2}$	0.96 (1.15)	0.78 (0.98)	0.60 (0.75)	0.29 (0.43)	0.10 (0.22)	-0.12 (0.03)
$\Delta E_{1,0}$	0.69 (0.64)	0.59 (0.56)	0.41 (0.36)	0.23 (0.18)	0.13 (0.10)	0.11 (0.13)

the splittings but also the ordering of the levels for the spin doublets. In fact, the inversion of levels appears, in Fig. 3, as seen in the results of the first-excited doublet ($1_2^-, 2_1^-$) for the NSC97f at $\rho_\Sigma = 1$ and 2 though the splitting energies are very small.

Tzeng *et al.* have shown that the 1^- states for both of the doublets become more attractive compared to the other spin partners if they take into account the effect of the Λ - Σ coupling three-body force [4]. In our approach, the effect of the Λ - Σ three-body force is automatically taken into account when we include the ΣN channel in the model space, as discussed before. In our results the trend of the Λ - Σ three-body effect on the first-excited doublet agrees with the results by them, but that on the ground-state doublet does not necessarily agree for the NSC97f.

We should say, however, that the Λ - Σ three-body effect

on the energy levels may appear more clearly if we use a YN potential which has a strong ΣN - ΛN interaction such as the NSC89 potential. As a matter of fact, both splittings of the doublets become larger as ρ_Σ increases, if we use the NSC89. For example, the splitting energies of the ground-state doublet are 0.17MeV and 0.61MeV, respectively, for the cases of “ ΛN ” and $\rho_\Sigma = 5$, and those of the first-excited doublet, 0.26MeV and 0.81MeV. We note here that both of the 1^- states are always more attractive than the other spin partners for the NSC89 regardless of the values of ρ_Σ , which is a different feature from the results for the NSC97 models. Our results of the two doublets for the NSC89 agree fairly well with their results [4].

In Table II, the calculated energies of the low-lying states for $\rho_\Sigma = 5$ are tabulated for the NSC97a-f potentials. The results for “ ΛN ” are also shown in paren-

theses for reference. Smooth variation of the splittings of the ground and first-excited doublets with negative parity is observed when we change the YN potentials from the NSC97a to NSC97f. It may be considered that this variation is a reflection of the different strengths of the spin-dependent interactions originated from the variation of the magnetic $F/(F+D)$ ratio α_V^m for the vector mesons in the NSC97a-f [16]. The gradual change can be also seen in the Λ spin-orbit splitting in ${}^{17}_\Lambda\text{O}$ as shown in Table I. We note that the 1^-_1 state of the ground-state doublet lies in energy above the 0^-_1 state for the NSC97a-f.

In the E930 experiment at BNL, two γ -transitions from the 1^-_2 state to the ground-state doublet ($0^-_1, 1^-_1$) are expected to be observed [8]. From these the magnitude of the splitting of the ground-state doublet should be established. Our results might help to constrain parameters such as α_V^m for the NSC97 models in determining YN interactions.

As for the positive parity states, one can see that the calculated results have very weak dependence on ρ_Σ for the NSC97d and NSC97f in Fig. 3. It has been confirmed that similar tendency is observed for the other NSC97 models. In Table II, the calculated energies of the positive- and negative-parity states have been tabulated for the NSC97a-f potentials. In Fig. 4, we also show the calculated energy levels using the NSC97a-f and NSC89 potentials for $\rho_\Sigma = 5$ together with the experimental lev-

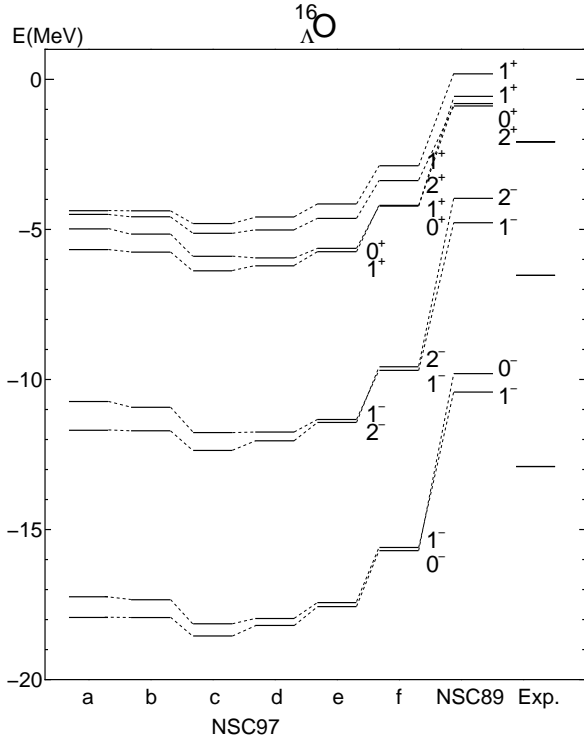


FIG. 4: Energy levels in ${}^{16}_\Lambda\text{O}$. The calculated results were obtained for $\rho_\Sigma = 5$. The experimental levels were taken from Ref. [23].

els.

An interesting feature can be seen concerning the relative position of the 0^+_1 and 2^+_1 states. Our results of the 0^+_1 state are below the 2^+_1 state in energy, except for the NSC89. The relative positions of the 0^+_1 and 2^+_1 states in our results show a different feature from the results of the shell-model calculations by other groups [4, 5] though the same YN interactions are employed. In those calculations, the 2^+_1 state lies below the 0^+_1 state. In a simple picture, the 0^+_1 and 2^+_1 states have the main components composed of $[0p_{1/2}^\Lambda, 0p_{1/2}^{-1}]$ and $[0p_{3/2}^\Lambda, 0p_{1/2}^{-1}]$, respectively. Thus, the 2^+_1 state should be below the 0^+_1 state in connection with the positions of the $0p_{3/2}^\Lambda$ and $0p_{1/2}^\Lambda$ states which are separated in energy by the Λ spin-orbit splitting in ${}^{17}_\Lambda\text{O}$.

We found that the inversion of the levels in our results was caused mainly by the parity-mixing intershell coupling in $1\hbar\omega$ excitation as discussed by Motoba [5]. As a unique feature of the structure of Λ hypernuclei, negative- and positive-parity nuclear core states can couple in the same energy region through a transition of Λ states such as the $0p_{1/2}^\Lambda$ state to the $0s_{1/2}^\Lambda$ state. In other words, even if the $1p$ - $1\hbar$ excitation of nuclear core pushes its energy up by about $1\hbar\omega$, the energy can be compensated by the transition of Λ states in $1\hbar\omega$ energy region. In our calculation using the NSC97f and the Paris potentials, the 0^+_1 state does not have the simple $[0p_{1/2}^\Lambda, 0p_{1/2}^{-1}]$ configuration, but a rather complex structure, as illustrated in Table III. We see that the probability for the last configuration which includes the positive-parity core-excited state is the same order of magnitude as that for the first configuration which includes the negative-parity state of the core nucleus.

As for the 2^+_1 state, however, such a strong effect of the parity-mixing intershell coupling does not appear. The dominant configuration is only $[0p_{3/2}^\Lambda, 0p_{1/2}^{-1}]$ which is the natural configuration with the lowest unperturbed energy. It should be noted that the 2^+_1 state can not be con-

TABLE III: The percentage analysis of the low-lying positive parity states for $\rho_\Sigma = 5$. The percentage for each configuration denotes the probability, namely, the square of mixing amplitude. The values in parentheses denote the results using the renormalized “ ΛN ” effective interaction. The NSC97f and the Paris potentials are employed for the YN and NN interactions, respectively.

Configuration	0^+_1	1^+_1	2^+_1
$[0p_{1/2}^\Lambda, 0p_{1/2}^{-1}]$	30.1%	1.9%	0%
	(27.4%)	(1.8%)	(0%)
$[0p_{3/2}^\Lambda, 0p_{1/2}^{-1}]$	0%	37.8%	65.6%
	(0%)	(34.3%)	(64.0%)
$[0s_{1/2}^\Lambda, 0s_{1/2}^{-1}]$	12.1%	9.0%	0%
	(12.3%)	(9.5%)	(0%)
$[0s_{1/2}^\Lambda, 0d_{5/2}^{-1}, 0p_{3/2}^{-1}, 0p_{1/2}^{-1}]$	33.0%	26.6%	6.9%
	(35.8%)	(30.2%)	(8.4%)

structed from the configurations including the $0s_{1/2}^{\Lambda}$ state in the space of the 1Λ - $1h$ configuration. The $[0s_{1/2}^{\Lambda}, 0s_{1/2}^{-1}]$ configuration can couple with the p - h excited configuration $[0s_{1/2}^{\Lambda}, 0d_{5/2}, 0p_{3/2}^{-1}, 0p_{1/2}^{-1}]$ through the NN effective interaction to construct the 0_1^+ state. Thus, the energies of the 0_1^+ and 2_1^+ states are dependent on the adopted NN interaction as well as the YN interaction. The same discussion on the parity-mixing intershell coupling as the 0_1^+ state applies to the 1_1^+ state as we see from Table III. Although the parity-mixing intershell coupling also affects the 2_1^+ state, the effect is considerably smaller than the 0_1^+ and 1_1^+ states. Therefore, we conclude that the parity-mixing intershell coupling strongly affects special states such as the 0_1^+ and 1_1^+ states with the help of the NN effective interaction.

Concerning the comparison with the experimental levels, we may say that the calculated results of the excitation spectra from the ground state agree well with the experimental values, on the whole, as shown in Fig. 4. The relative energy between the lowest two levels in the experimental data corresponds to the spin-orbit splitting energy of the nucleon. Our results of the splitting between the lowest two bunched levels show a good agreement with the corresponding experimental values. These splittings of the calculated results are obtained, reflecting the property of the adopted NN interaction which is the Paris potential in the present study.

In the present shell-model calculations, we do not employ the experimental single-particle energies of Λ , Σ , and nucleons. The results thus obtained show directly the differences in properties between the YN interactions. In general, the effective YN and NN interactions are derived dependently on the single-particle energies of Λ , Σ , and nucleons. These single-particle energies are determined by both of the spin-dependent and spin-independent interactions. In this context, our results reflect not only the spin-dependent interaction but also the spin-independent one of the free YN and NN interactions.

We here make some comments on the results obtained by Tzeng *et al.* [4, 24]. It seems that our results of $^{16}_{\Lambda}\text{O}$ considerably differ from their results at first sight. As a matter of fact, the dependence of the calculated energy levels in the absolute value on the YN interactions is different from each other. This is mainly because of the difference of the treatment of the single-particle energies. In their method, a common set of the semi-empirical single-particle energies is employed in the calculations using various YN interactions. Therefore, there are considerable differences in the absolute values of the energy levels between their and our results. However, as far as we are concerned with the excitation spectra, especially the splittings of the two doublets with negative parity, our results of $^{16}_{\Lambda}\text{O}$ for the NSC97a-f and NSC89 potentials are consistent, on the whole, with the results obtained by them. As a general feature, our results of the splittings of the two doublets show a little smaller values than

their results.

We move to the discussion on the dependence of the calculated results on the YN interactions. In our results of the ground-state doublet in $^{16}_{\Lambda}\text{O}$, the result for the NSC97c is the most attractive in the NSC97 models, and that for the NSC97f is the least attractive. One may consider that this tendency is not consistent with results of $^4_{\Lambda}\text{He}$ in a recent calculation [25]. In that study, the binding energy of the ground 0^+ state for the NSC97f is the most attractive, and the result for the NSC97d is the least attractive. Results for the NSC97a-c potentials have not been given in their paper. This question of the inconsistency can be solved by analyzing matrix elements of our ΛN effective interaction.

In Fig. 5, some of the representative matrix elements of the renormalized “ ΛN ” effective interaction for the NSC97 models are shown. We see that the matrix elements vary almost linearly from the NSC97a to NSC97f. In the shell-model language, the dominant contribution of the matrix element to the ground 0^+ state in $^4_{\Lambda}\text{He}$ should be $\langle 0s_{1/2}0s_{1/2} | \tilde{v}_{\Lambda N} | 0s_{1/2}0s_{1/2} \rangle_{J=0}$, namely, the spin-singlet s -wave interaction. This matrix element for the NSC97f is the most attractive in the NSC97 models as seen in Fig. 5, and the dependence on the YN interactions is consistent with the results of $^4_{\Lambda}\text{He}$. On the other hand, the matrix element $\langle 0s_{1/2}0s_{1/2} | \tilde{v}_{\Lambda N} | 0s_{1/2}0s_{1/2} \rangle_{J=1}$ which represents the spin-triplet s -wave interaction contributes dominantly to the 1^+ state, namely, the spin partner of the 0^+ state in $^4_{\Lambda}\text{He}$. The value of this matrix element for the NSC97f is the least attractive in the NSC97 models. This trend is observed in their results of the 1^+ state in

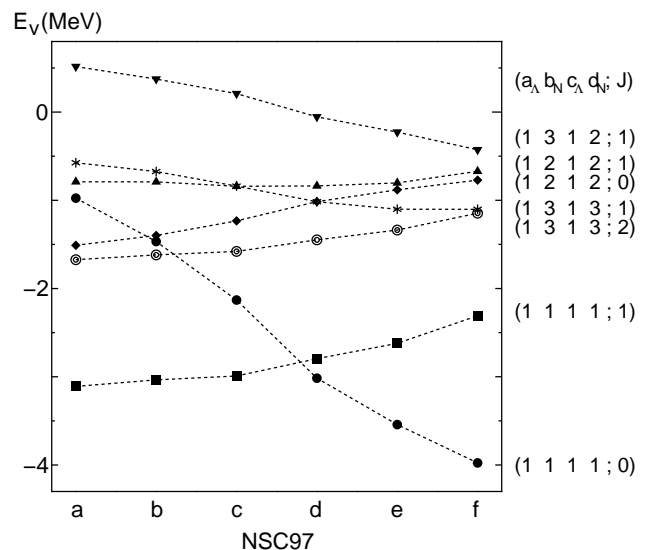


FIG. 5: Dependence of some of the representative matrix elements of the renormalized “ ΛN ” effective interaction $\langle a_{\Lambda} b_N | \tilde{v}_{\Lambda N} | c_{\Lambda} d_N \rangle_{J,T=1/2}$ on the NSC97 models in $^{16}_{\Lambda}\text{O}$. The single-particle states are labeled as $1 = 0s_{1/2}$, $2 = 0p_{1/2}$, and $3 = 0p_{3/2}$.

${}^4_\Lambda\text{He}$ [25]. Therefore, our results are not inconsistent with the results of ${}^4_\Lambda\text{He}$.

In the calculation of the ground-state doublet with negative parity in ${}^{16}_\Lambda\text{O}$, the other matrix elements in Fig. 5 are important. These matrix elements include effects of the p -wave interaction in addition to the s -wave one. The p -wave interaction also contributes to the Λ single-particle energy for the $0s_{1/2}$ state, and thus the structure of ${}^{16}_\Lambda\text{O}$ becomes more complex than ${}^4_\Lambda\text{He}$. As a result, the energies for the NSC97c are the most attractive in the NSC97 models in ${}^{16}_\Lambda\text{O}$. It may be considered that the study of ${}^{16}_\Lambda\text{O}$ is useful to investigate properties of higher partial-wave interactions such as the p -wave interaction.

Finally, we move back to the discussion on the comparison of our results and the experimental values. Roughly speaking, the experimental energy levels lie between the two results for the NSC97f and NSC89 potentials. As we mentioned before, however, effects of the many-body effective interaction are not included in the present calculation. In the previous study, the effect of the three-body cluster (TBC) terms on the Λ single-particle energy in ${}^{17}_\Lambda\text{O}$ was investigated [10]. It was confirmed that the TBC terms caused a repulsive contribution of about 1MeV to the Λ single-particle energy for the $0s_{1/2}$ state in ${}^{17}_\Lambda\text{O}$ for the NSC97f. This suggests that the TBC effect shifts the energy levels of the negative-parity states in ${}^{16}_\Lambda\text{O}$ repulsively to the same extent, if we take into account this effect in the present study. Thus, the NSC97f potential might be favorable in the NSC97 models for the calculation for ${}^{16}_\Lambda\text{O}$.

IV. CONCLUDING REMARKS

Shell-model calculations for ${}^{17}_\Lambda\text{O}$ and ${}^{16}_\Lambda\text{O}$ in a large model space have been performed. By introducing a new model space including ΣN states, we have calculated effective interactions which include the ΣN - ΛN coupling terms. As far as we know, the degrees of freedom of Σ in addition to Λ and nucleons have been explicitly introduced in the shell-model calculations for the first time. The effective interactions and the single-particle energies employed in the shell-model calculations have been microscopically derived from the NSC97a-f and NSC89 YN interactions and the Paris NN interaction within the framework of the UMOA.

It has been confirmed that the results of the present shell-model diagonalization for ${}^{17}_\Lambda\text{O}$ with the NSC97a-f potentials agree well with those of our previous study in which the calculation was performed perturbatively. The Λ spin-orbit splitting energies obtained are 0.44MeV to 0.95MeV for the NSC97a to NSC97f. These values seem to be considerably larger than the value suggested from the experimental result of ${}^{13}_\Lambda\text{C}$ which has been established recently.

It has been found that a drastic change in the structure of ${}^{16}_\Lambda\text{O}$ induced by the Σ degrees of freedom does not occur as far as we employ the NSC97a-f potentials. The

Σ degrees of freedom give rise to a small effect on the first-excited doublet ($1^-_2, 2^-_1$) in ${}^{16}_\Lambda\text{O}$. However, if we use the NSC89 potential which has a strong ΣN - ΛN interaction, the splittings of the ground and first-excited doublets, respectively, ($0^-_1, 1^-_1$) and ($1^-_2, 2^-_1$) are enlarged. The magnitude of the splitting of the ground-state doublet gradually decreases as 0.69MeV to 0.11MeV from the NSC97a to NSC97f. We should note that the 0^-_1 state lies below the 1^-_1 state in energy for the NSC97 models. On the other hand, the 1^-_1 state is below the 0^-_1 state for the NSC89. In the E930 experiment at BNL, the magnitude of the ground-state doublet should be determined in the near future, which would give useful information on the underlying properties of the YN interaction.

Effects of the parity-mixing intershell coupling on $1\hbar\omega$ excited states have been investigated. It has been found that the parity-mixing intershell coupling plays an important role in the structure of the 0^+_1 and 1^+_1 states in ${}^{16}_\Lambda\text{O}$ with the help of the NN effective interaction. As a result, the 0^+_1 and 1^+_1 states have complex structures. On the other hand, the parity-mixing intershell coupling on the 2^+_1 state is less active than the 0^+_1 and 1^+_1 states.

In conclusion, the present shell-model results, especially, the excitation spectra have shown a good agreement with the experimental levels on the whole, even though our calculation method is fully microscopic and does not include any experimental values and adjustable parameters. The experimental levels are between the two results for the NSC97f and NSC89. In the near future, some fine structures of Λ hypernuclei reflecting the properties of the underlying YN interaction would be revealed experimentally. We hope that our method will help to bridge between the YN interaction and the Λ hypernuclear structure microscopically, and give useful constraint to determine YN interactions more realistically.

Acknowledgments

The authors are grateful to Yiharn Tzeng for the calculations for ${}^{16}_\Lambda\text{O}$ using the NSC97a-e potentials in reply to our request. One of the authors (S. F.) would like to thank H. Tamura for useful discussion about the E930 experiment at BNL. He also acknowledges the Special Postdoctoral Researchers Program of RIKEN.

APPENDIX A: MATRIX ELEMENTS OF ΛN EFFECTIVE INTERACTIONS

In Table IV, we tabulate representative matrix elements of the renormalized “ ΛN ” effective interactions for the NSC97a-f potentials for reference. The “ ΛN ” means that the ΣN channel is not included in the model space in determining the “ ΛN ” effective interactions. The results using these potentials are tabulated in parentheses in Tables I and II, and shown in Figs. 2 and 3. The matrix elements in the $0s$ and $0p$ shells are given.

TABLE IV: Matrix elements of the renormalized “ ΛN ” effective interaction $\langle a_\Lambda b_N | \tilde{v}_{\Lambda N} | c_\Lambda d_N \rangle_{J,T=1/2}$ for the NSC97a-f potentials. The single-particle states are labeled as $1 = 0s_{1/2}$, $2 = 0p_{1/2}$, and $3 = 0p_{3/2}$. All energies are in MeV.

a_Λ	b_N	c_Λ	d_N	J	NSC97a	NSC97b	NSC97c	NSC97d	NSC97e	NSC97f
1	1	1	1	0	-0.975	-1.467	-2.130	-3.016	-3.542	-3.976
1	1	1	1	1	-3.109	-3.035	-2.991	-2.795	-2.621	-2.308
1	2	1	2	0	-1.510	-1.398	-1.233	-1.015	-0.881	-0.771
1	2	1	2	1	-0.790	-0.791	-0.841	-0.837	-0.803	-0.671
1	3	1	2	1	0.516	0.374	0.209	-0.054	-0.227	-0.427
1	3	1	3	1	-0.574	-0.674	-0.839	-1.016	-1.101	-1.102
1	3	1	3	2	-1.673	-1.619	-1.579	-1.448	-1.337	-1.146
2	1	1	2	0	-1.583	-1.617	-1.727	-1.750	-1.713	-1.538
2	1	1	2	1	0.990	0.917	0.817	0.658	0.554	0.449
2	1	1	3	1	-1.170	-1.306	-1.477	-1.702	-1.832	-1.950
2	2	1	1	0	-0.083	-0.274	-0.536	-0.883	-1.088	-1.247
2	2	1	1	1	0.301	0.260	0.261	0.202	0.133	-0.019
2	3	1	1	1	-1.087	-1.052	-1.018	-0.931	-0.865	-0.761
2	1	2	1	0	-1.783	-1.677	-1.531	-1.317	-1.177	-1.037
2	1	2	1	1	-1.170	-1.188	-1.258	-1.277	-1.255	-1.129
2	2	2	2	0	0.243	0.166	0.013	-0.140	-0.211	-0.178
2	2	2	2	1	-1.271	-1.222	-1.200	-1.098	-1.002	-0.823
2	3	2	2	1	-0.208	-0.223	-0.227	-0.243	-0.260	-0.300
2	3	2	3	1	-1.040	-0.961	-0.872	-0.715	-0.605	-0.452
2	3	2	3	2	-1.142	-1.201	-1.294	-1.382	-1.419	-1.406
3	1	1	2	1	1.298	1.434	1.603	1.823	1.950	2.062
3	1	1	3	1	-0.118	0.051	0.272	0.588	0.784	0.969
3	1	1	3	2	1.433	1.414	1.410	1.353	1.295	1.195
3	2	1	1	1	1.087	1.052	1.018	0.931	0.865	0.761
3	3	1	1	0	-0.117	-0.388	-0.757	-1.249	-1.538	-1.764
3	3	1	1	1	-1.163	-1.105	-1.075	-0.961	-0.858	-0.669
3	1	2	1	1	-0.563	-0.402	-0.211	0.089	0.286	0.507
3	2	2	2	1	0.273	0.287	0.283	0.297	0.314	0.363
3	2	2	3	1	0.947	0.956	0.986	0.982	0.961	0.903
3	2	2	3	2	-0.659	-0.569	-0.457	-0.283	-0.169	-0.050
3	3	2	2	0	-0.371	-0.648	-0.986	-1.471	-1.771	-2.070
3	3	2	2	1	0.933	0.914	0.919	0.886	0.843	0.754
3	3	2	3	1	-0.934	-0.913	-0.898	-0.848	-0.805	-0.735
3	3	2	3	2	0.145	0.245	0.371	0.551	0.663	0.780
3	1	3	1	1	-0.646	-0.779	-0.986	-1.221	-1.342	-1.378
3	1	3	1	2	-1.920	-1.863	-1.822	-1.681	-1.561	-1.352
3	2	3	2	1	-0.950	-0.865	-0.764	-0.597	-0.486	-0.344
3	2	3	2	2	-1.084	-1.138	-1.228	-1.310	-1.343	-1.324
3	3	3	2	1	0.974	0.949	0.932	0.878	0.829	0.749
3	3	3	2	2	-0.171	-0.275	-0.402	-0.586	-0.702	-0.824
3	3	3	3	0	-0.043	-0.315	-0.707	-1.203	-1.485	-1.662
3	3	3	3	1	-0.923	-0.849	-0.809	-0.670	-0.549	-0.323
3	3	3	3	2	-0.308	-0.352	-0.430	-0.505	-0.540	-0.523
3	3	3	3	3	-1.738	-1.703	-1.686	-1.597	-1.514	-1.368

- [1] Jifa Hao, T. T. S. Kuo, A. Reuber, K. Holinde, J. Speth, and D. J. Millener, Phys. Rev. Lett. **71**, 1498 (1993); *ibid.* **74**, 4762 (1995).
- [2] T. T. S. Kuo and E. Osnes, *Folded-Diagram Theory of the Effective Interaction in Nuclei, Atoms and Molecules*, Lecture Notes in Physics, Vol. 364 (Springer, Berlin, 1990).
- [3] Yiharn Tzeng, S. Y. Tsay Tzeng, T. T. S. Kuo, and T.-S. H. Lee, Phys. Rev. C **60**, 044305 (1999).
- [4] Yiharn Tzeng, S. Y. Tsay Tzeng, T. T. S. Kuo, T.-S. H. Lee, and V. G. D. Stoks, Phys. Rev. C **61**, 031305 (2000).
- [5] T. Motoba, Nucl. Phys. **A639**, 135c (1998).
- [6] R. H. Dalitz, D. H. Davis, T. Motoba, and D. N. Tovee, Nucl. Phys. **A625**, 71 (1997).
- [7] H. Bandō and Y. Yamamoto, Prog. Theor. Phys. Suppl. **81**, 9 (1985).
- [8] H. Tamura, Nucl. Phys. **A691**, 86c (2001).
- [9] S. Fujii, R. Okamoto, and K. Suzuki, Nucl. Phys. **A651**, 411 (1999); *ibid.* **A676**, 475 (2000).
- [10] S. Fujii, R. Okamoto, and K. Suzuki, Prog. Theor. Phys.

- 104**, 123 (2000).
- [11] K. Suzuki, R. Okamoto, and H. Kumagai, Phys. Rev. C **36**, 804 (1987); K. Suzuki and R. Okamoto, Prog. Theor. Phys. **92**, 1045 (1994).
- [12] K. Suzuki and S. Y. Lee, Prog. Theor. Phys. **64**, 2091 (1980).
- [13] P. Navrátil, J. P. Vary, and B. R. Barrett, Phys. Rev. Lett. **84**, 5728 (2000); P. Navrátil and W. E. Ormand, Phys. Rev. Lett. **88**, 152502 (2002).
- [14] N. Barnea, W. Leidemann, and G. Orlandini, Nucl. Phys. **A693**, 565 (2001).
- [15] P. M. M. Maessen, Th. A. Rijken, and J. J. de Swart, Phys. Rev. C **40**, 2226 (1989).
- [16] Th. A. Rijken, V. G. J. Stoks, and Y. Yamamoto, Phys. Rev. C **59**, 21 (1999).
- [17] A. Reuber, K. Holinde, and J. Speth, Nucl. Phys. **A570**, 543 (1994).
- [18] S. Ajimura *et al.*, Phys. Rev. Lett. **86**, 4255 (2001).
- [19] T. Yamada, T. Motoba, K. Ikeda, and H. Bando, Prog. Theor. Phys. Suppl. **81**, 104 (1985).
- [20] K. Suzuki and R. Okamoto, Prog. Theor. Phys. **76**, 127 (1986).
- [21] M. Lacombe, B. Loiseau, J. M. Richard, R. Vinh Mau, J. Côté, P. Pirès, and R. de Tournel, Phys. Rev. C **21**, 861 (1980).
- [22] D. J. Millener, A. Gal, C. B. Dover, and R. H. Dalitz, Phys. Rev. C **31**, 499 (1985); D. J. Millener, Nucl. Phys. **A691**, 93c (2001).
- [23] H. Tamura, R. S. Hayano, H. Oota, and T. Yamazaki, Prog. Theor. Phys. Suppl. **117**, 1 (1994).
- [24] Yiharn Tzeng, private communication, (2002).
- [25] A. Nogga, H. Kamada, and W. Glöckle, Phys. Rev. Lett. **88**, 172501 (2002).